

Full Length Research Paper

Magneto hydrodynamic (MHD) squeezing flow of a Casson fluid between parallel disks

Naveed Ahmed¹, Umar Khan¹, Sheikh Irfanullah Khan^{1,2}, Yang Xiao-Jun³, Zulfiqar Ali Zaidi^{1,2} and Syed Tauseef Mohyud-Din¹

¹Department of Mathematics, Faculty of Sciences, HITEC University, Taxila Cantt, Pakistan.

²COMSATS Institute of Information Technology, University Road, Abbottabad, Pakistan.

³College of Science, China University of Mining and Technology, Xuzhou, Jiangsu, 221008, China.

Accepted 20 September, 2013

Squeezing flow of a Casson fluid is considered between two parallel disks. Upper disk is taken to be impermeable but capable of moving towards or away from the lower fixed and porous disk. Governing equations are derived with the help of conservation laws combined with suitable similarity transforms. Homotopy analysis method (HAM) is then been employed to determine the solution to resulting ordinary differential equation. Numerical solution is also obtained using R-K 4 method and comparison shows an excellent agreement between both solutions. Effects of different physical parameters on the flow are also discussed with the help of graphs along with comprehensive discussions.

Key words: Casson fluid, homotopy analysis method (HAM), squeezing flow, parallel disks, magneto hydrodynamic (MHD) flow, numerical solution.

INTRODUCTION

Squeezing flow between parallel disks has been an active field of research. Its biological and industrial applications have attracted many researchers towards its study. Numbers of efforts have been made to understand such types of flows in more depth. Motion of pistons is vital for running engines and machines. Squeezing flow under the influence of moving disk is also involved in nasogastric tubes and syringes. Better understanding of these flows leads us to more efficient and effective machines which may be used for both industrial and biological purposes.

After the foundational directions provided by Stefan (1874), many researchers investigated the squeezing flow problems (Reynolds, 1886; Archibald, 1956; Grimm, 1976; Wolfe, 1965; Kuzma, 1968; Tichy and Winer, 1970; Jackson, 1962; Hughes and Elco, 1962). As in most of

the cases fluids under consideration are non-Newtonian hence due to complex nature of these fluids different mathematical models are used to study their flow. For blood type fluids Mill et al. (1965) and McDonald (1974) depicted a most compatible model known as Casson fluid.

Later Domairry and Aziz (2009) considered the flow of an electrically conducting fluid between two parallel disks of which lower disk is permeable and fluid can enter or exit through it during suction or injection process; upper disk is taken to be impermeable and it moves towards the lower disk with a certain time dependent velocity. They applied homotopy perturbation method (HPM) to approximate the solution. Due to inherent nonlinearities in Navier Stokes equations, exact solution in most of the cases is unlikely, therefore, different approximation

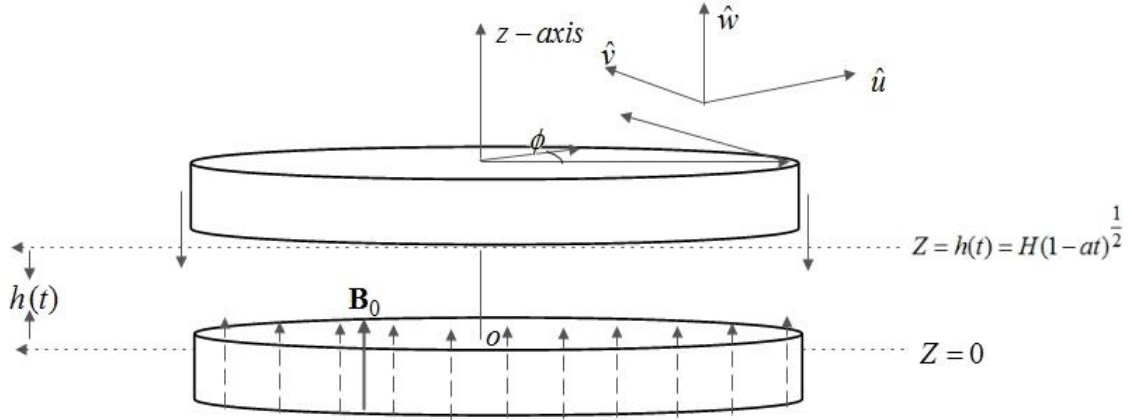


Figure 1. Schematic diagram of the problem.

techniques are used to approximate the solution analytically (Abbasbandy, 2007a, b; Abdou and Soliman, 2005a; Noor and Mohyud-Din, 2007; Abdou and Soliman, 2005b; Asadullah et al., 2013; Noor et al., 2008; Mohyud-Din et al., 2009; Nadeem et al., 2012). One of these analytical methods is homotopy analysis method (HAM) that has been effectively applied by different researchers to various nonlinear problems (Liao, 2003; Liao, 2004; Abbasbandy and Zakaria, 2008; Abbasbandy, 2007c; Tan and Abbasbandy, 2008; Hussain et al., 2012; Zeeshan et al., 2012; Hayat et al., 2003; Hayat et al., 2004; Khan et al., 2008; Hayat et al., 2009; Ellahi et al., 2010; Ellahi, 2013; Ellahi, 2012; Ellahi et al., 2012; Hayat et al., 2006).

In this paper, squeezed flow of magneto hydrodynamic (MHD) flow of a non-Newtonian Casson fluid is presented. The governing nonlinear partial differential equations are reduced to a much simpler nonlinear ordinary differential equation by employing a similarity transform. The reduced equation is solved by HAM and effects of emerging parameters are demonstrated graphically coupled with comprehensive discussions. A numerical solution is also carried out by using Runge-Kutta fourth order method to check the validity of analytical solution. An excellent agreement among the solutions is observed.

MATHEMATICAL ANALYSIS

Consider MHD incompressible flow of a Casson fluid between parallel infinite disks separated by a distance $h(t) = H(1 - at)^{1/2}$. A magnetic field proportional to

$B_0(1 - at)^{1/2}$ is applied perpendicular to the disks. Based on the assumption of low Reynolds number, the induced magnetic field is neglected. The upper disk at $z = h(t)$ is moving with velocity $\frac{aH(1 - at)^{-1/2}}{2}$ towards or away from the stationary lower disk at $z = 0$. The physical configuration is presented in Figure 1. Rheological equation of Casson fluid is defined as follows (Nadeem et al., 2012):

$$\tau_{ij} = \left[\mu_B + \left(\frac{p_y}{2\pi} \right)^{1/n} \right]^n 2e_{ij}, \tag{1}$$

μ_B is dynamic viscosity of the non-Newtonian fluid, p_y is yield stress of fluid and π is the product of component of deformation rate with itself, that is, $\pi = e_{ij}e_{ij}$, where e_{ij} is the (i, j) th component of the deformation rate.

We have chosen the cylindrical coordinates system (r, ϕ, z) . Due to the rotational symmetry of the flow ($\partial/\partial\phi = 0$), the azimuthal component v of the velocity $V = (u, v, w)$ vanishes identically. Thus, the governing equation for unsteady two-dimensional flow and heat transfer of a Casson fluid are:

$$\frac{\partial \hat{u}}{\partial r} + \frac{\hat{u}}{r} + \frac{\partial \hat{w}}{\partial z} = 0 \tag{2}$$

$$\rho \left(\frac{\partial \hat{u}}{\partial t} + \hat{u} \frac{\partial \hat{u}}{\partial r} + \hat{w} \frac{\partial \hat{u}}{\partial z} \right) = - \frac{\partial \hat{p}}{\partial r} + \mu \left(1 + \frac{1}{\beta} \right) \left(2 \frac{\partial^2 \hat{u}}{\partial r^2} + \frac{2}{r} \frac{\partial \hat{u}}{\partial r} + \frac{\partial^2 \hat{u}}{\partial z^2} + \frac{\partial^2 \hat{u}}{\partial r \partial z} - 2 \frac{\hat{u}}{r^2} \right) - \frac{\sigma}{\rho} B^2(t) \hat{u} \tag{3}$$

$$\rho \left(\frac{\partial \hat{w}}{\partial t} + \hat{u} \frac{\partial \hat{w}}{\partial r} + \hat{w} \frac{\partial \hat{w}}{\partial z} \right) = - \frac{\partial \hat{p}}{\partial z} + \mu \left(1 + \frac{1}{\beta} \right) \left(\frac{\partial^2 \hat{w}}{\partial r^2} + 2 \frac{\partial^2 \hat{w}}{\partial z^2} + \frac{1}{r} \frac{\partial \hat{w}}{\partial r} + \frac{1}{r} \frac{\partial \hat{u}}{\partial z} + \frac{\partial^2 \hat{u}}{\partial z^2} \right) \tag{4}$$

The boundary conditions are (Domairry and Aziz, 2009):

$$\begin{aligned} \hat{u} = 0, \quad \hat{w} = \frac{dh}{dt} \quad \text{at } z = h(t) \\ \hat{u} = 0, \quad \hat{w} = -w_0 \quad \text{at } z = 0. \end{aligned} \tag{5}$$

In the above equations, \hat{u} and \hat{w} are the velocity components in the r - and z - directions respectively, ρ is density, μ dynamic viscosity, \hat{p} pressure, ν kinematic viscosity and w_0 is the suction/injection velocity.

Substituting the following transformations (Domairry and Aziz, 2009):

$$\begin{aligned} \hat{u} = \frac{ar}{2(1-at)} f'(\eta), \quad \hat{w} = - \frac{aH}{\sqrt{1-at}} f'(\eta), \\ B(t) = \frac{B_0}{\sqrt{1-at}}, \quad \eta = \frac{z}{H\sqrt{1-at}}. \end{aligned} \tag{6}$$

into Equations 2 and 3 and eliminating the pressure gradient from the resulting equations, we finally obtain

$$\begin{aligned} f_{n+1}(\eta) = A + \frac{1}{2} A_1 \eta^2 + \frac{1}{6} A_2 \eta^3 \\ - \left(\frac{\beta+1}{\beta} \right) \int_0^\eta (\eta-s)^3 \left(-S(3f_n''(s) + sf_n''(s)) - 2f_n(s)f_n''(s) \right) ds, \\ \left(-M^2 f_n(s)f_n''(s) \right) ds, \end{aligned} \tag{7}$$

with the boundary conditions

$$\begin{aligned} f(0) = A, \quad f'(0) = 0, \\ f(1) = \frac{1}{2}, \quad f'(1) = 0. \end{aligned} \tag{8}$$

Where S denotes the squeeze number, A the suction/blowing parameter and M is the Hartman number, defined as:

$$S = \frac{aH^2}{2\nu}, \quad M^2 = \frac{aB_0^2 H^2}{\nu}. \tag{9}$$

SOLUTION PROCEDURE

Zero order deformation problem

Following the procedure proposed by Liao (2003), it is forthright to choose following initial guess:

$$f_0(\eta) = A + \frac{1}{2} (3-6A)\eta^2 + (-1+2A)\eta^3. \tag{10}$$

Linear operator is selected as:

$$L_f = \frac{df^4}{d\eta^4}. \tag{11}$$

Above operator satisfies the following property:

$$L_f (C_1 + C_2\eta + C_3\eta^2 + C_4\eta^3) = 0, \tag{12}$$

where $C_i (i=1-4)$ are the constants. Zero order deformation problem can now be constructed as follows (Noor et al., 2008):

$$(1-q)L_f[\tilde{f}(\eta, q) - f_0(\eta)] = qhN_f[\tilde{f}(\eta, q)], \tag{13}$$

$$\tilde{f}(0, q) = A, \quad \tilde{f}'(0, q) = 0, \quad \tilde{f}(1, q) = \frac{1}{2}, \quad \tilde{f}'(1, q) = 0, \tag{14}$$

where $q \in [0,1]$ is an embedding parameter and h is nonzero auxiliary parameter. Nonlinear operator is

$$\begin{aligned} N_f[\tilde{f}(\eta, q)] \\ = \frac{\partial^4 \tilde{f}(\eta, q)}{\partial \eta^4} - \left(\frac{\beta}{1+\beta} \right) \left\{ S \left(\eta \frac{\partial^3 \tilde{f}(\eta, q)}{\partial \eta^3} + 3 \frac{\partial^2 \tilde{f}(\eta, q)}{\partial \eta^2} - 2\tilde{f}(\eta, q) \frac{\partial^3 \tilde{f}(\eta, q)}{\partial \eta^3} \right) \right. \\ \left. - M^2 \frac{\partial^2 \tilde{f}(\eta, q)}{\partial \eta^2} \right\}. \end{aligned} \tag{15}$$

For $q=0$ and $q=1$ we have

$$\tilde{f}(\eta, 0) = f_0(\eta), \quad \tilde{f}(\eta, 1) = f(\eta). \tag{16}$$

$\tilde{f}(\eta, p)$ can be expressed as a Taylor's series in terms of q , that is,

$$\tilde{f}(\eta, q) = f_0(\eta) + \sum_{m=1}^{\infty} f_m(\eta) q^m, \quad f_m(\eta) = \frac{1}{m!} \left. \frac{\partial^m f(\eta, q)}{\partial q^m} \right|_{q=0}. \tag{17}$$

Substituting $q=1$ in above equation we obtain

$$\tilde{f}(\eta, 1) = f_0(\eta) + \sum_{m=1}^{\infty} f_m(\eta). \tag{18}$$

m^{th} -order deformation problem

m times differentiation of zero order problem depicted by Equation 13 and setting $q=0$ leads to

$$L_f[\tilde{f}_m(\eta) - \chi_m f_{m-1}] = h\mathcal{R}_m^f(\eta), \tag{19}$$

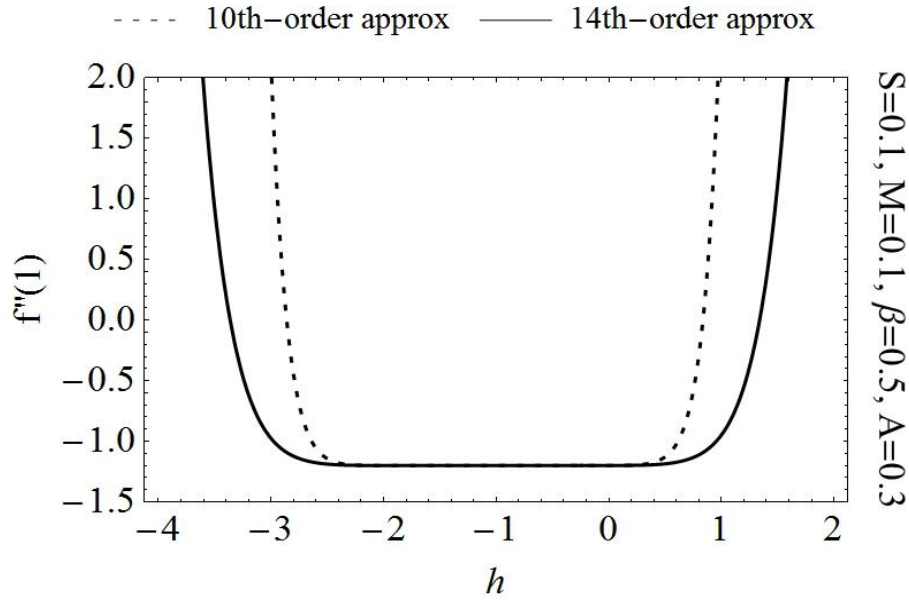


Figure 2. *h* curves for the function *f* for different orders of approximations.

Where

$$\mathfrak{R}_m^f(\eta) = f_{m-1}''' - \left(\frac{\beta}{1+\beta}\right) \left\{ S(\eta f_{m-1}''' + 3f_{m-1}'') - M^2 f_{m-1}' + 2S \sum_{k=0}^{m-1} f_{m-1-k} f_k'' \right\} \quad (20)$$

$$\mathcal{X}_m = \begin{cases} 0, & m \leq 1 \\ 1, & m > 1 \end{cases} \quad (21)$$

The general solution of Equation 19 is

$$f_m(\eta) = f_m^\circ(\eta) + C_1^m + C_2^m \eta + C_3^m \eta^2 + C_4^m \eta^3, \quad (22)$$

where $f_m^\circ(\eta)$ represents the special solution; also

$$\begin{aligned} C_1^m &= -f_m^\circ(0), & C_2^m &= -\left. \frac{\partial f_m^\circ(\eta)}{\partial \eta} \right|_{\eta=0} \\ C_3^m &= -3C_1 - 2C_2 - 3f_m^\circ(1) + \left. \frac{\partial f_m^\circ(\eta)}{\partial \eta} \right|_{\eta=1} \\ C_4^m &= 2C_1 + C_2 + 2f_m^\circ(1) - \left. \frac{\partial f_m^\circ(\eta)}{\partial \eta} \right|_{\eta=1} \end{aligned} \quad (23)$$

Above higher order solution can be substituted to Equation 18 to obtain the final solution.

Convergence of the solution

Obtained series solution given by Equation 18 contains an auxiliary parameter *h*. As pointed out by Liao (2003), this parameter is the

key to control convergence of series solution. Acceptable range of *h* can be determined by identifying the line segment of so called *h*-curves which is parallel to *h* axis. In our particular problem this can be achieved by seeing the range in which $f''(1)$ bears the same magnitude for any value of *h* within that range. Figure 2 is displayed to demonstrate convergence region for two orders of approximations namely 10th and 14th. It clearly shows that the acceptable region of *h* is to be between -2.4 and 0.4.

RESULTS AND DISCUSSION

Acceptable range for auxiliary parameter *h* has been discussed in previous section. In our analysis and discussions we use $h = -0.9$ as an optimal value of *h*. After ensuring the convergence of series solution our concern now is to see the influences of suction/blowing parameter *A*, squeeze number *S*, Hartmann number *M* and Casson fluid parameter β on velocity is examined. For convenience, we divide our discussions into two parts; one dedicated to investigate the upshots on varying physical parameter for the case suction ($A > 0$) and the other one describes the same effects for the case of blowing ($A < 0$).

Suction case

Effects of increasing suction at lower disk on both axial and radial velocities are displayed in Figures 3 and 4

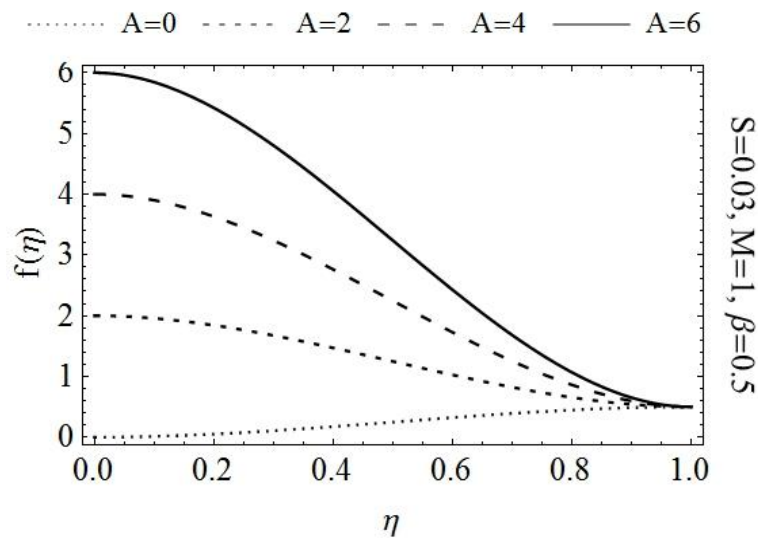


Figure 3. Effects of A on axial velocity.

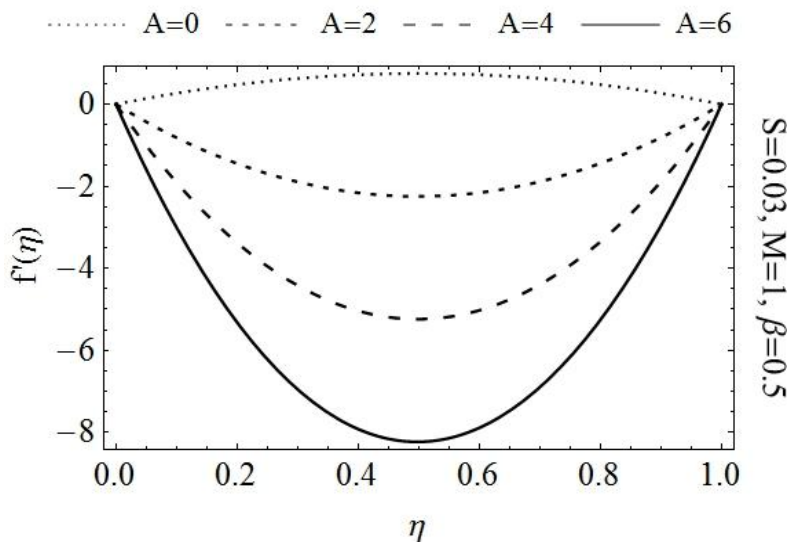


Figure 4. Effect of A on radial velocity.

respectively. It is evident that increasing value of A results in higher absolute values of both the velocities. As increasing suction allows more fluid to flow near the lower disk therefore a decrease in boundary layer thickness is expected.

Influences of squeeze parameter S on axial and radial velocities are displayed in Figures 4 and 5 respectively. Here $S < 0$ corresponds to the movement of upper disk towards lower one. On the other hand, $S > 0$ describes away movement of the same disk. It can be seen from Figure 5 that for squeezing motion of upper disk

combined with suction axial velocity near the center is increased while for dilating motion a decrease in axial velocity is observed. From Figure 6 one can see the behavior of radial velocity for same variations in S. It is evident for expanding motion; an accelerated radial flow is observed near the upper disk however this trend changes gradually as we move away from it. Somewhere near the center this trend gets converted into an opposite one; that is, from that point to lower disk a delayed motion is observed. For contracting motion of upper disk combined with suction at lower disk effects of increasing

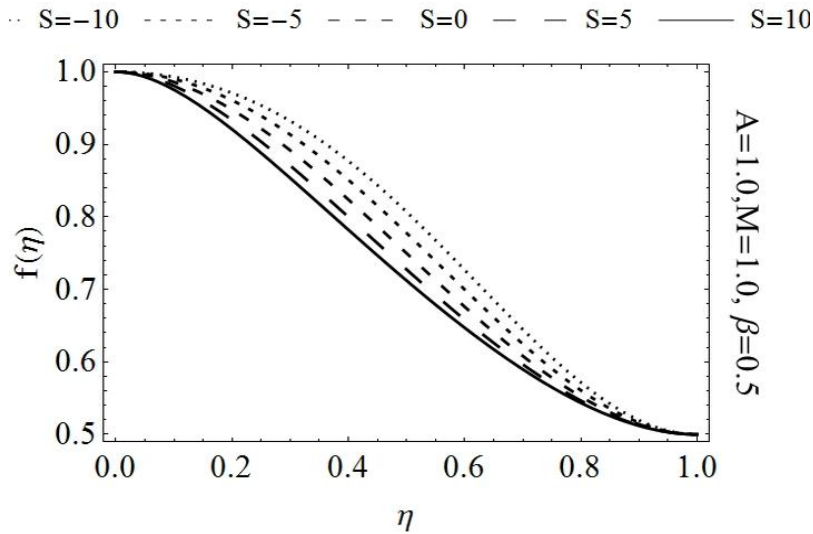


Figure 5. Effects of S on axial velocity.

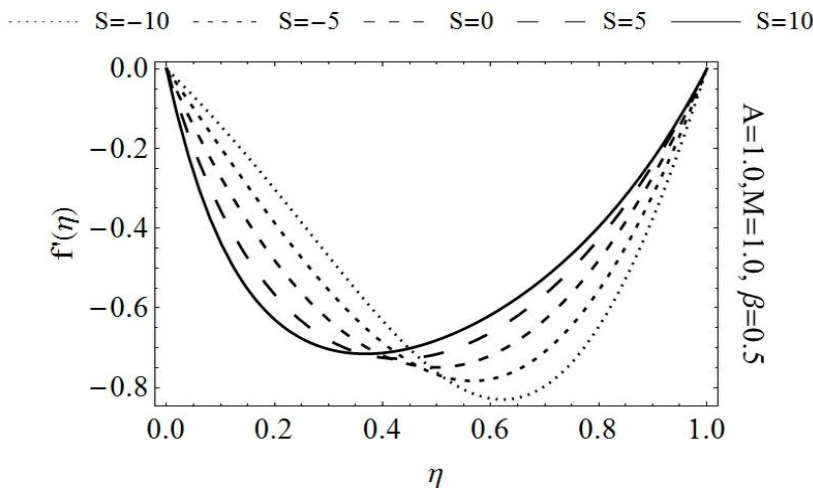


Figure 6. Effect of S on radial velocity.

absolute values of S are quite opposite to the case of expanding motion. In this case, radial velocity near upper disk decreases while near the lower disk an accelerated radial flow is observed.

Graphical results describing flow behavior under increasing Hartmann number M are displayed in Figures 7 and 8. From Figure 7, it can be seen that the axial velocity $f(\eta)$ is a decreasing function of M . As apparent from Figure 8, absolute value of radial velocity $f'(\eta)$ increases near the disks while in center, it behaves oppositely. It is also worth mentioning that effect near upper disk is more prominent as compared to lower one. Figures 9 and 10 respectively are dedicated to display

behavior of axial and radial velocity for increasing Casson parameter β . Axial velocity is a decreasing function of β as shown in Figure 9. Effects of β on axial velocity are more visible in central region as compared to the area near disks. Furthermore, $\beta \rightarrow \infty$ gives us the flow of viscous fluid. Figure 10 shows that the radial velocity near lower disk decreases with rising β . However, after moving some distance away from the lower disk this behavior changes into an opposite one; that is, after $\eta > 0.4$ we observe an accelerated radial flow. One may also see that effects of β near the disks are very slight as compared to the region far from them.

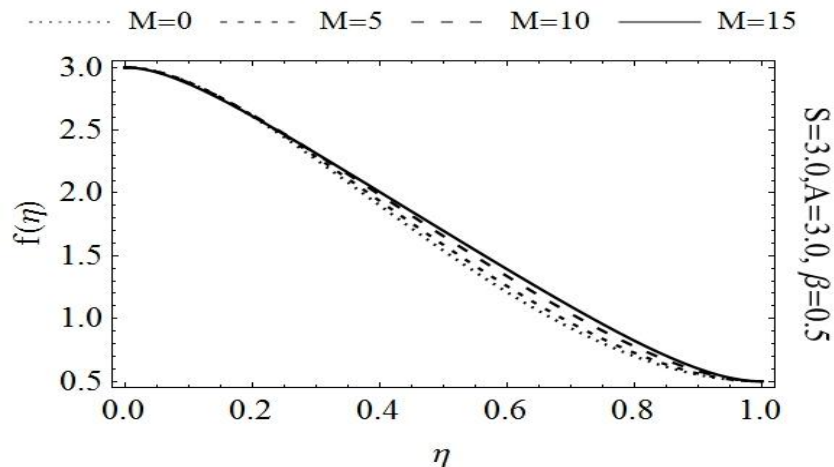


Figure 7. Effects of M on axial velocity.

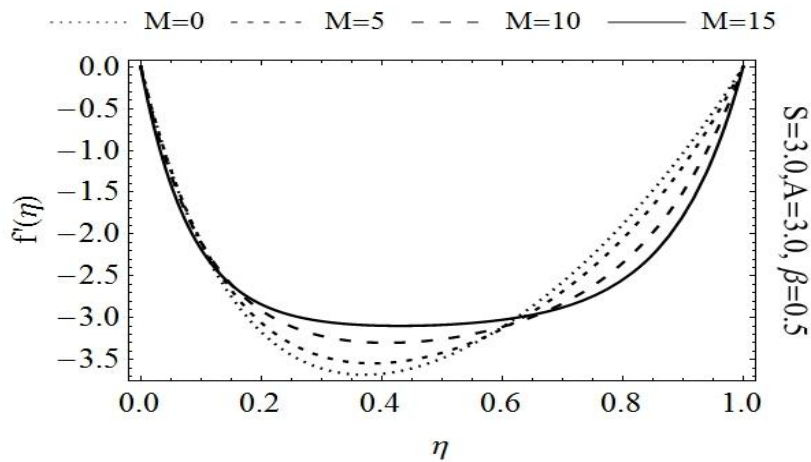


Figure 8. Effect of M on radial velocity.

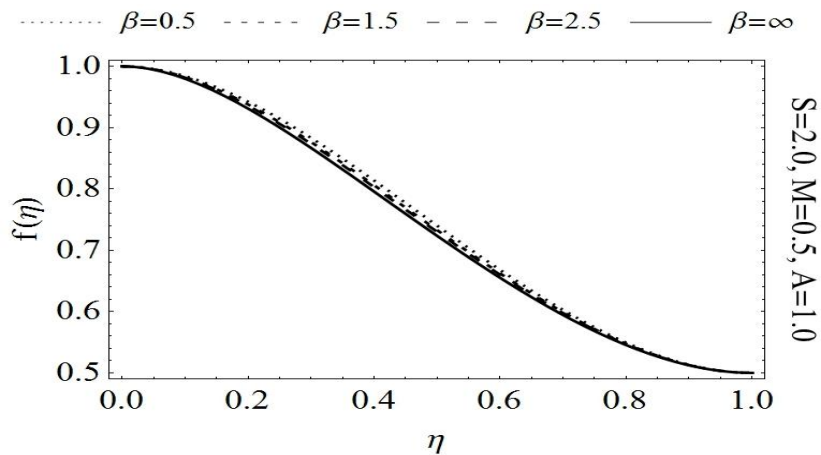


Figure 9. Effects of β on axial velocity.

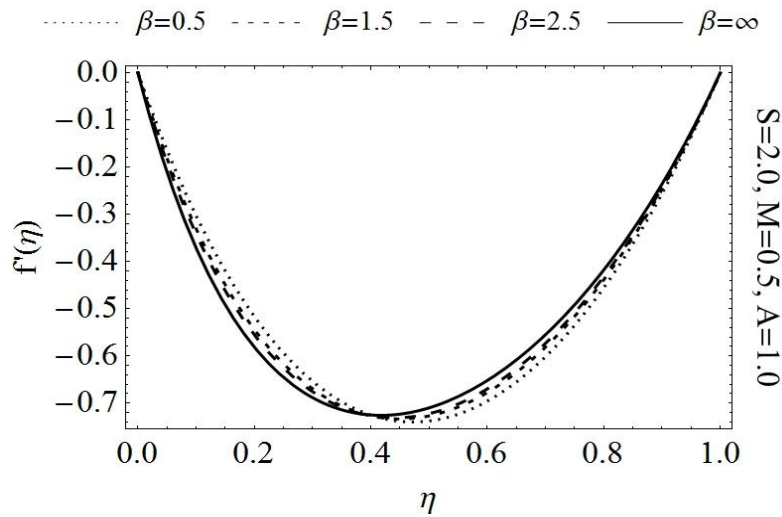


Figure 10. Effect of β on radial velocity.

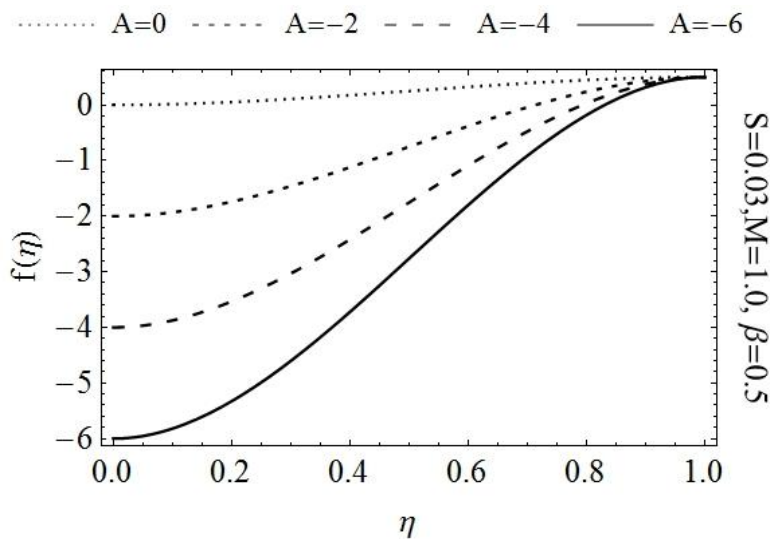


Figure 11. Effects of A on axial velocity.

Blowing case

Here we discuss influences of involved physical parameter in the case when blowing occurs at the lower disk. Figures 11 and 12 declare that the influence on increasing injection leads to increased absolute values of both axial and radial velocities. Figures 13-18 show that the effects of S , M and β on both axial and radial flow are opposite in blowing case as compared to the ones obtained for suction case. Same problem is solved numerically by using a well-known RK-4 method. Comparison for is presented in Table 1. It can be observed that both

numerical and analytical solutions are in excellent agreement.

Conclusion

Squeezing flow between parallel disks is presented. Homotopy analysis method (HAM) has been employed to obtain analytical solution to the problem. Influences of emerging flow parameters are discussed in detail with the help of graphs. It is also concluded that the effects of physical parameter on axial and radial velocities are quite

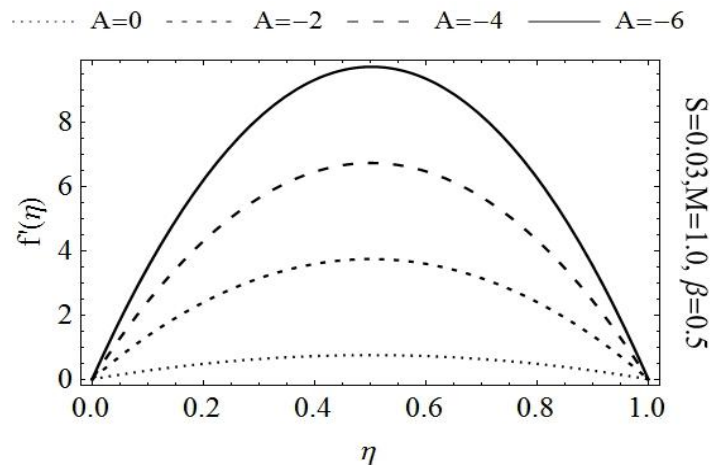


Figure 12. Effect of A on radial velocity.

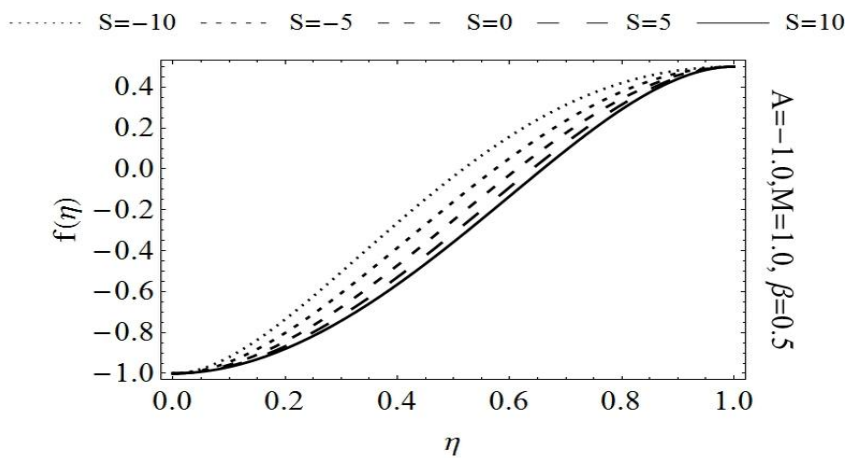


Figure 13. Effects of S on axial velocity.

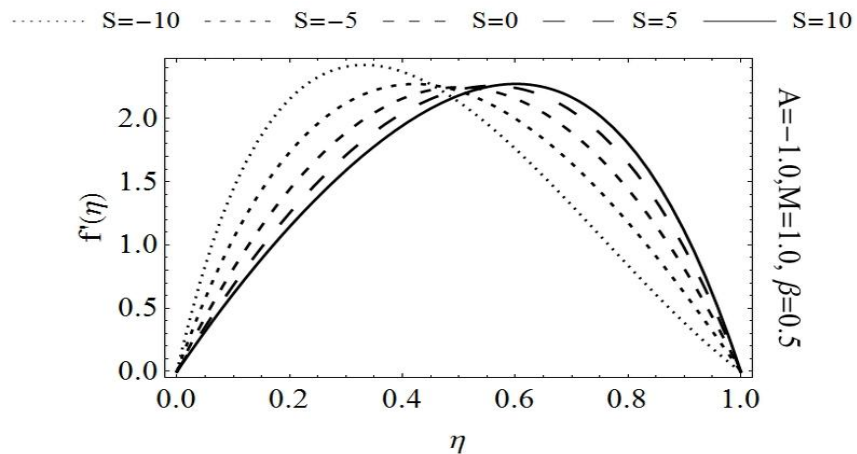


Figure 14. Effect of S on radial velocity.

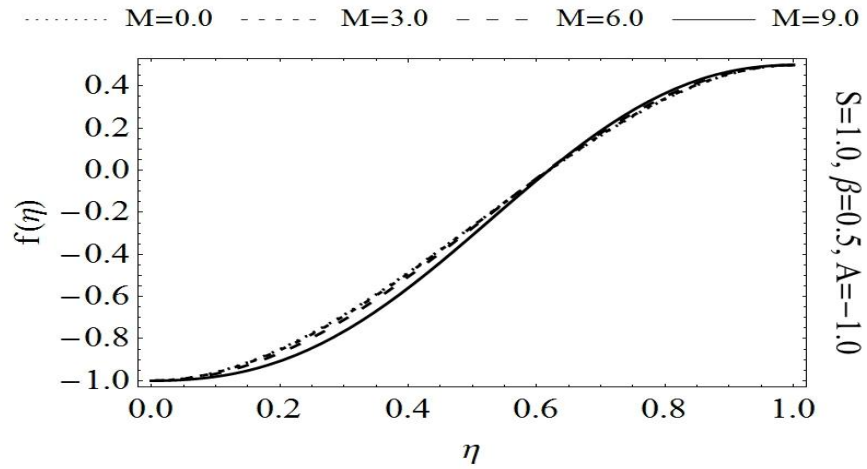


Figure 15. Effects of M on axial velocity.

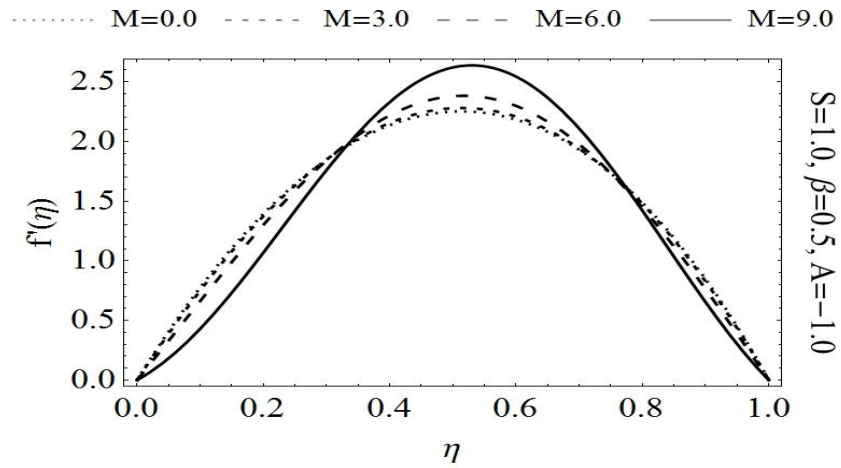


Figure 16. Effect of M on radial velocity.

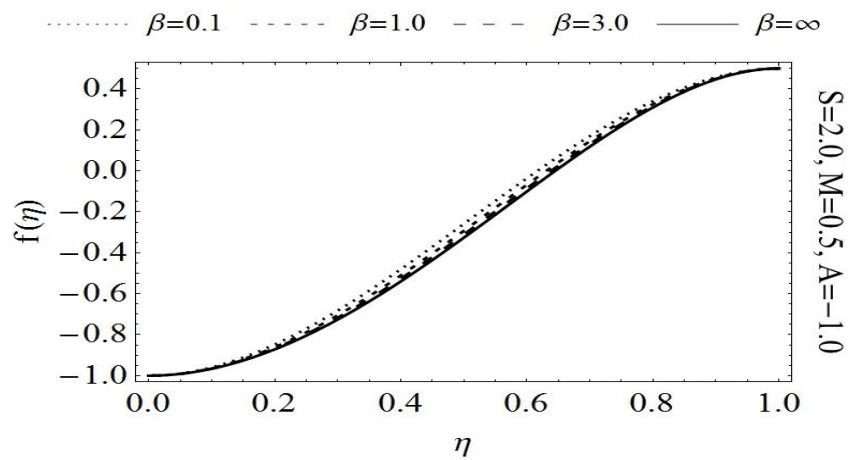


Figure 17. Effects of β on axial velocity.

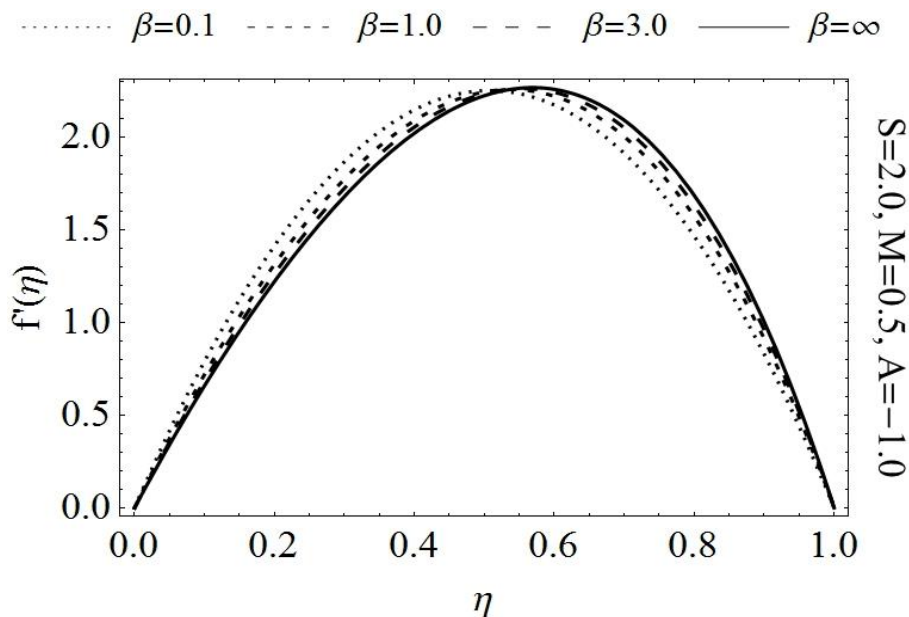


Figure 18. Effect of β on radial velocity.

Table 1. Comparison of HAM and numerical solutions for $S = 2.0, A = 1.0, M = 0.5, h = -0.9, \beta = 0.5$.

η	$f(\eta)$ HAM	Numerical	$f'(\eta)$ HAM	Numerical
0	1.000000	1.000000	0	0
0.1	0.984012	0.984012	-0.303368	-0.303368
0.2	0.942321	0.942321	-0.516753	-0.516753
0.3	0.883192	0.883192	-0.654099	-0.654099
0.4	0.813695	0.813695	-0.725515	-0.725515
0.5	0.740051	0.740051	-0.737995	-0.737995
0.6	0.667911	0.667911	-0.695962	-0.695962
0.7	0.602598	0.602598	-0.601667	-0.601667
0.8	0.549306	0.549306	-0.455454	-0.455454
0.9	0.513283	0.513283	-0.255919	-0.255919
1.0	0.500000	0.500000	0	0

opposite in the cases of suction to the blowing. A numerical solution using well known R-K 4 method has also been obtained for the sake of comparison. It is found that the results agree exceptionally well.

REFERENCES

Abbasbandy S (2007a). The application of homotopy analysis method to solve a generalized Hirota-Satsuma coupled KdV equation, Phys. Lett. A. 361:478–483.
 Abbasbandy S (2007b). A new application of He's variational iteration method for quadratic Riccati differential equation by using Adomian's polynomials, J. Computational Appl. Math. 207:59-63.

Abbasbandy S (2007c). Numerical solutions of nonlinear Klein-Gordon equation by variational iteration method, Int. J. Num. Methods Eng. 70:876-881.
 Abbasbandy S, Zakaria FS (2008). Soliton solutions for the fifth-order K-dV Equation with the homotopy analysis method, Nonlinear Dynamics, 51:83–87.
 Abdou MA, Soliman AA (2005a). New applications of variational iteration method, Physica D. 211(1-2):1-8.
 Abdou MA, Soliman AA (2005b). Variational iteration method for solving Burger's and coupled Burger's equations. J. Computational Appl. Math. 181:245-251.
 Archibald FR (1956). Load capacity and time relations for squeeze films. J. Lubrication Technol. 78:A231–A245.
 Asadullah M, Khan U, Ahmed N, Manzoor R, Mohyud-Din ST (2013). Int. J. Modern Math. Sci. 6:92-106.
 Domairy G, Aziz A (2009). Approximate Analysis of MHD Squeeze Flow

- between Two Parallel Disks with Suction or Injection by Homotopy Perturbation Method, *Mathematical Problems in Engineering*, article ID/2009/603916.
- Ellahi R (2012). A Study on the Convergence of Series Solution of Non-Newtonian Third Grade Fluid with Variable Viscosity: By Means of Homotopy Analysis Method, *Adv. Math. Phys.* Article ID 634925, 11 pages.
- Ellahi R (2013). The effects of MHD and temperature dependent viscosity on the flow of non-Newtonian nanofluid in a pipe: Analytical solutions, *Appl. Math. Modeling*, 37:1451-1467.
- Ellahi R, Hayat T, Mahomed FM, Zeeshan A (2010). analytical solutions for MHD flow in an annulus, *Commun. Nonlin. Sci. Numer. Simul.* 15:1224-1227.
- Ellahi R, Raza M, Vafai K (2012). Series solutions of non-Newtonian nanofluids with Reynolds' model and Vogel's model by means of the homotopy analysis method, *Mathe. Computer Modelling*, 55:1876–1891.
- Grimm RJ (1976). Squeezing flows of Newtonian liquid films: an analysis includes the fluid inertia. *Appl. Sci. Res.* 32(2):149–166,
- Hayat T, Ellahi R, Ariel PD, Asghar S (2006). Homotopy Solution for the Channel Flow of a Third Grade Fluid, *Nonlinear Dynamics*, 45:55–64.
- Hayat T, Ellahi R, Asghar S (2004). Unsteady periodic flows lows of a magnetohydrodynamic fluid due to noncoaxial rotations of a porous disk and a fluid at infinity, *Math. Computer Modelling*, 40:173-179.
- Hayat T, Ellahi R, Mahomed FM (2009). The Analytical Solutions for Magnetohydrodynamic Flow of a Third Order Fluid in a Porous Medium, *Zeitschrift Naturforsch*, 64a:531-539.
- Hayat T, Mumtaz S, Ellahi R (2003). MHD unsteady periodic flows due to non-coaxial rotations of a disk and a fluid at infinity, *Acta Mathematica Sinica*, 19:235-240.
- Hughes WF, Elco RA (1962). Magnetohydrodynamic lubrication flow between parallel rotating disks. *J. Fluid Mechanics*, 13:21–32.
- Hussain A, Mohyud-Din ST, Cheema TA (2012). Analytical and Numerical Approaches to Squeezing Flow and Heat Transfer between Two Parallel Disks with Velocity Slip and Temperature Jump, *Chinese Phys. Lett.* 29:114705.
- Jackson JD (1962). A study of squeezing flow, *Appl. Sci. Res. A.* 11:148–152.
- Khan I, Ellahi R, Fetecau C (2008). Some MHD Flows of a Second Grade Fluid through the Porous Medium. *J. Porous Media*, 11:389-400.
- Kuzma DC (1968). Fluid inertia effects in squeeze films. *Appl. Sci. Res.* 18:15–20.
- Liao SJ (2003). Beyond perturbation: introduction to the Homotopy Analysis Method, CRC Press, Boca Raton, Chapman and Hall, 2003.
- Liao SJ (2004). On the homotopy analysis method for nonlinear problems, *Appl. Math. Computation*, 147:499–513.
- McDonald DA (1974). *Blood Flows in Arteries*, 2nd ed. Arnold, London
- Mohyud-Din ST, Noor MA, Waheed A (2009). Variation of parameter method for solving sixth-order boundary value problems, *Communication Korean Math. Soc.* 24:605-615.
- Mrill EW, Benis AM, Gilliland ER, Sherwood TK, Salzman EW (1965). Pressure flow relations of human blood hollow fibers at low flow rates. *J. Appl. Physiol.* 20:954–967.
- Nadeem S, Haq UIR, Lee C (2012). MHD flow of a Casson fluid over an exponentially shrinking sheet, *Scientia Iranica*, 19:1150-1553.
- Noor MA, Mohyud-Din ST (2007). Variational iteration technique for solving higher order boundary value problems, *Appl. Math. Computation*, 189:1929-1942.
- Noor MA, Mohyud-Din ST, Waheed A (2008). Variation of parameters method for solving fifth-order boundary value problems. *Appl. Math. Infor. Sci.* 2:135 -141.
- Reynolds O (1886). On the theory of lubrication and its application to Mr. Beauchamp Tower's experiments, including an experimental determination of the viscosity of olive oil, *Philosophical Transactions of the Royal Society of London*, 177:157–234.
- Stefen MJ (1874). Versuch" Uber die scheinbare adhesion, *Sitzungsberichte der Akademie der Wissenschaften in Wien. Mathematik-Naturwissen*, 69:713–721.
- Tan Y, Abbasbandy S (2008). Homotopy analysis method for quadratic Riccati differential Equation, *Communications Nonlinear Sci. Num. Simulation*, 13:539–546.
- Tichy JA, Winer WO (1970). Inertial considerations in parallel circular squeeze film bearings, *J. Lubrication Technol.* 92:588–592.
- Wolfe WA (1965). Squeeze film pressures. *Appl. Sci. Res.* 14:77–90.
- Zeeshan A, Ellahi R, Siddiqui AM, Rahman HU (2012). An investigation of porosity and magnetohydrodynamic flow of non-Newtonian nanofluid in coaxial cylinders, *Int. J. Phys. Sci.* 7(9):1353–1361.